Available online at http://jess.esrae.ru/

"Journal of Economics and Social Sciences"

Analysis of plasmonic nanoparticles applications and their influence on scattered electric field

Tomsk Polytechnic University

Andrey Averkiev[a]

[a] Research School of Chemistry & Applied Biomedical Sciences

Abstract

It is known that plasmon-induced photocatalytic reaction can may occur due to the excitation of electrons on the surface of plasmonic nanoparticles (NP) but there are also other ways due to which a «hot electron» transfer reaction and a photocatalytic reaction are possible. Nowadays, there are several reports that highlight possible methods of various applications of photocatalytic reactions.
The first aim of this report is to analyze excited researches about different mechanisms of photocatalysis and their implications in medicine to find out new approach in cancer treatment available for every person in society, and diagnostics. The second aim is to show nanosphere 3D simulation results of enhancement and electric field dependents of irradiation light wavelength, and size of NP. Also, this review is highlighting some investigation methods of plasmon-induced photocatalytic reaction at the micro and nanoscale.

Keywords: Photocatalysis, nanoparticles, therapy, diagnostics, plasmon-induced, nanoscale;

1. Introduction

Plasmons consisting of free electrons oscillation on the surface of noble metals led to the discovery of many new phenomena in nanophotonics over the past two decades, which contributed to promising applications in surface spectroscopy and plasmon photocatalysis. Such effects arise from local field amplification or from plasmon-induced hot carriers. It is very desirable to fit the excitement. That is why we should always consider wavelength of irradiation light because all metallic NP require different wavelength of plasmon resonance to reach excitation maximum and electric field (EF) enhancement and its distribution around. So optimal gain or efficiency can be achieved in the following various applications [13].

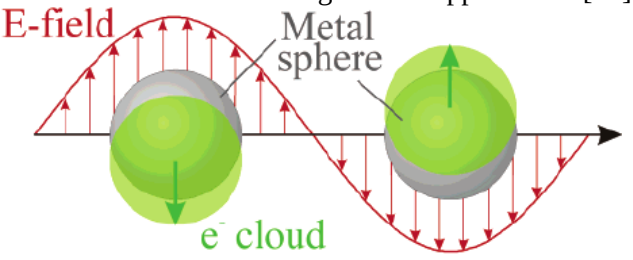

Figure 1. Schematic image of plasmon oscillation for a sphere showing the displacement of the electron conduction charge cloud relative to the nuclei [11].

2. Materials and methods

The authors of this report [13] carried out light-induced rearrangement of bound plasmons by expanding the nanogaps by in situ polymerization. To establish the initial clearance, the Au substrate is coated with a 0.6-nm-thick self-assembled thiophenol monolayer, after which 80 nm Au nanoparticles are applied on top. This mirror of Au nanoparticles (NPoM) restricts strong optical fields (several hundred times greater than the incidence field) inside the nanogap [2]. The surface-bound plasmon mode of such plasmon structures is extremely sensitive to the size and content of the gap, which makes it possible to adjust the interval between nano-gaps on demand as well as accurately monitor the polymer growth around each gold nanoparticle. The initial color of coupled plasmon resonance from each NPoM is in the range of 10 nm from 800 nm showing a high degree of reliable construction of this architecture [1,3,4].

It was found that irradiation with a 635 nm continuous wave (CW) laser on these bulk Au NPoM monomers (0.2 mW /μm 2) divinylbenzene (DVB) increases the gap size. This leads to a 70 nm spectral shift (from 800 to 730 nm) bound plasmon resonance for 400 s (Fig. 2) [13].

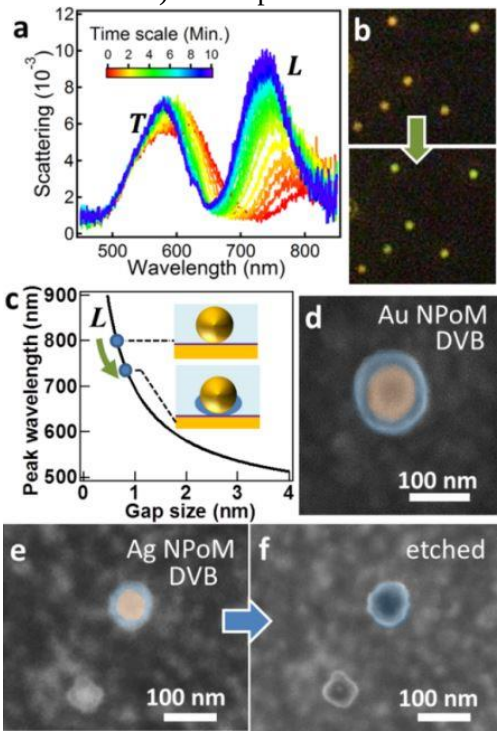

Figure 2. Using NPoM plasmon geometry to track light-induced polymerization of DVB. (a) Scattering spectra of Au NP on Au substrate vs irradiation time (635 nm 0.2 mW pump). T: transverse mode; L: dipolar mode. (b) Dark-field images of Au NPoMs before/after irradiation of entire area. (c) Circuit model prediction of coupled plasmon resonance (λL) vs gap size. Inset depicts polymer growth in the gap between Au NP and Au substrate. (d) SEM image of irradiated Au NPoM in DVB showing PDVB coating. (e, f) SEM images of irradiated Ag NPoM in DVB before/after etching Ag NPs with ammonia. Images are false-colored to highlight core−shell structure [13].

The method described in this report [13] can not only be used to remotely fine tune plasmons of NPoM nanostructures in an easy way but it also allows real-time monitoring and control of polymer growth using light. Although this method is not suitable for the mass production of polymers it is extremely versatile for synthesis in nanodevices combining selective local synthesis, fine tuning of sizes (<10 nm) and monitoring optical spectroscopy.

Various strategies use the optical properties of metal nanoparticles namely their ability to support localized surface plasmon resonances (LSPR). [9] The emerging paradigm that uses LSPR for photocatalysis is known as plasmon-mediated hot electron transfer (PHET), and an increasing number of reports demonstrate the ability of PHET to catalyze energy-complex chemical reactions [8,10,12]. This is an incredible opportunity to identify new classes of materials capable of providing the interaction of light with matter and energy transfer events that offer the same advantages as metal nanoparticles. They have the exceptional potential for the collection of light but also offer quite a big selectivity and efficiency in energy transfer as well as tunable surface chemistry to enhance catalytic activity.

This method [9] goes beyond the limits of perturbative inclusion of an electric field and allows us to follow the electronic degrees of freedom in strong fields with an arbitrary time dependence, which are characteristic of scattered absorption (SMA). In particular, the explicit time dependence of this approach allows us to fix transitions that become important since the near fields of scattering resonances continue to interact with metal electrons for 10–100 femtoseconds. During these time scales the population is accumulated in various excited configurations and transitions between different excited configurations become important for dynamics. This is a unique feature of SMA, which is probably not important in the plasmon generation of hot carriers due to the pulsed nature of the plasmon field.

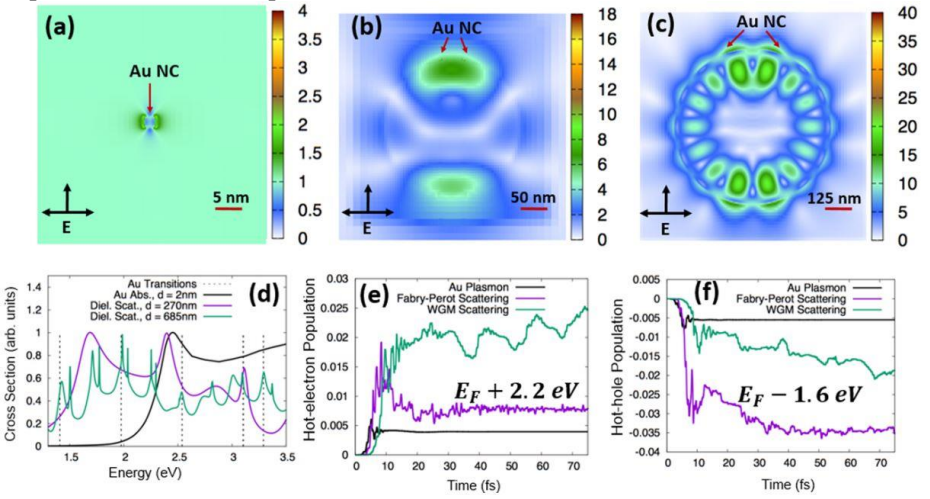

Figure 4. Three regimes for light−matter interactions leading to unique spatial and temporal shaping of the incident field and the corresponding impact on electronic dynamics in an L = 2 nm PIW Au nanocube. Plots of the near-field enhancements (|E|/|E0|) are shown for the Au NC LSPR (λ = 532 nm, panel a), a Fabry−Perot resonance of a d = 270 nm dielectric nanosphere decorated with Au NCs (λ = 397 nm, panel b), and a whispering gallery mode resonance of a d = 685 nm dielectric nanosphere decorated with Au NCs (λ = 493 nm, panel c). The extinction spectra of these three structures are shown overlaid with the dipole-allowed transitions in the PIW model of the Au NC showing particularly strong overlap between these transitions and the scattering resonances of the d = 685 nm dielectric nanosphere (panel d) [9].

The authors analyze the distribution and dynamics of hot carriers resulting from SMA and LSPR excitation by calculating the instantaneous populations of the orbitals both above and below the Fermi level of the metal nanostructure (Fig. 4) [9].

Surface Raman spectroscopy (SERS) is a unique optical phenomenon capable of improving the Raman signal of molecules by a factor of millions, which has attracted more and more attention over the past forty years. Electromagnetic (EM) amplification is one of two widely used SERS amplification mechanisms, which amplifies the Raman signal of probed molecules adjacent to a local electric field due to the surface plasmon resonance (SPR) effect. Here [5], a unique method is presented for improving the excitation and emission of SERS by developing an integrated Raman spectrometer (iPERS) using a specially developed aplanatic solid-state immersion lens (ASIL, NA ≈ 1.65) [5].

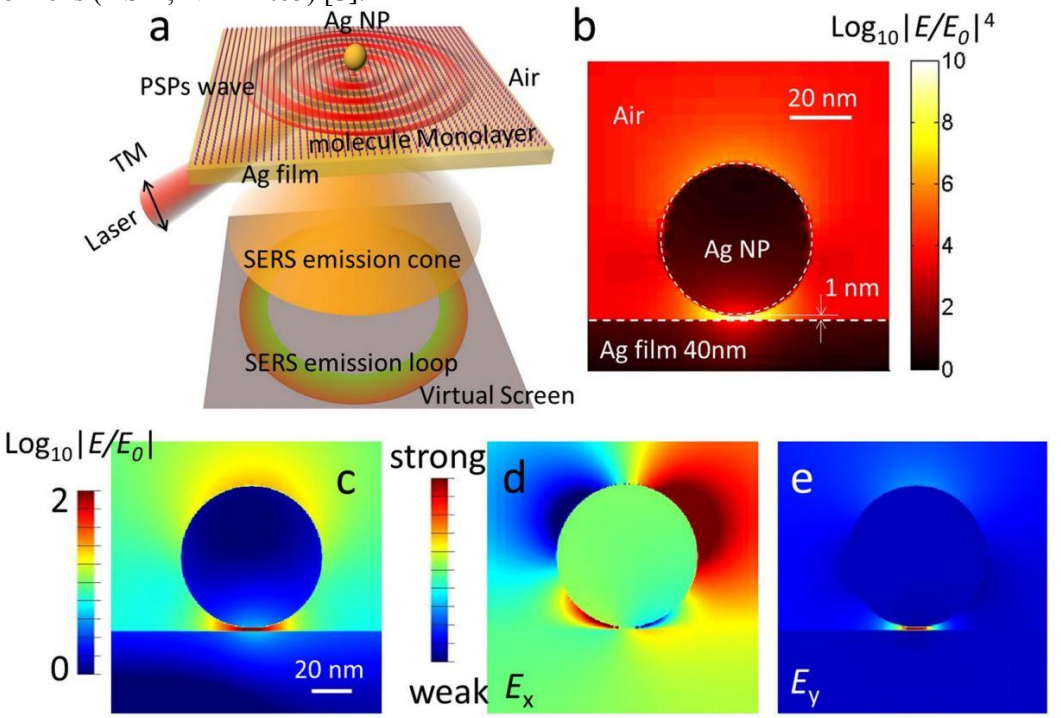

Figure 5. The excitation and emission of SERS in designed iPERS configuration and the local electric field enhancement from NOF substrate. (a) Schematic diagram of the directional excitation and emission of the SERS of the monomolecular layer located in the gap of an Ag NP-on-a film system (NOF). (b) SERS enhancement distribution of the NOF in near field simulated by three-dimensional finite-difference time domain (3D-FDTD) software. The NOF used in this research is constructed by an Ag NP (diameter: 50nm) over an Ag film (thickness: 40nm). The gap between the Ag NP and film is dependent on the thickness of the monomolecular layer located on the surface of the Ag film. Here, we set the gap as 1.0 nm according to the frequently probed molecules in SERS detections. The excitation laser is 785nm. (c) The electric field enhancement distribution of the NOF and its components in Ex (d) and Ey (e) simulated by 2D-FDTD software, showing the simultaneous excitation of quadrupole (d) and dipole (e) resonance modes [5].

Authors show that physical process in iPERS spectroscopy (shown in Figure 5a) involves two steps: (1) the coupling the localized surface plasmons (LSPs) in near field, and (2) the SERS

emission in far field. Firstly, the incident laser in p polarization (785nm) couples the propagating surface plasmons (PSPs) on an Ag film in a narrow angle range at which the transverse propagation vector of the incident laser matches PSPs. When the PSPs encounter an Ag NP on an Ag film the LSPs in the nanogap will be coupled. Secondly, the LSPs excite the Raman scattering of the probed molecules in the nanogap and the scattering light couples the PSPs of the Ag film again. Next, the PSPs radiate in far field along a certain cone angle according to the vector-match law. Thus, an emission loop comes out and a cone pattern of the SERS emission can be obtained in far field [7,14]. In this design, the coupling of LSPs in near field and the SERS emission in far field are integrated by an elaborately designed ASIL.

The EM fields in near and far fields were firstly estimated by finite difference time-domain (FDTD) simulation. An Ag NP (diameter: 50nm) on an Ag film (thickness: 40nm) configuration is excited by a 785-nm laser from the ASIL side. Under the resonance condition, a hot spot (shown as the red region) appears at the nanogap (1nm) in this NOF configuration. The SERS enhancement distribution in Fig. 5b shows the enhancement factor of SERS (|E/E0|4) reaches 10 orders of magnitude in the hot spot region. Figure 5c displays the electric field distribution of the NOF and its components in Ex and Ey (Fig. 5d and e), respectively. It can be found that quadrupole (Fig. 5d) and dipole (Fig. 5e) resonance modes can be simultaneously excited, which can answer for why such high EM field can be reached in the gap range in this NOF configuration [6].

3. Discussion

This part is mostly aimed to show 3D simulation results and investigation of it. These results are performed in COMSOL Multiphysics, wave optics module. Plane parallel waves with two wavelengths 550 and 650 were applied to Au nanoparticle with ideal spherical shape. This wave of light goes in two directions (Fig.6). The process of electromagnetic wave scattering takes place and due to this we can see enhancement of electric field around NPs. For 650 nm wavelength light goes along Z axis, from top to bottom (Fig.6 A). That is why we can observe the horizontal polarization of EF and its maximum intensity of $3.56*10^4$ V/m. In the second situation (Fig. 6 B) the wave of 550 nm length is settled on the X axis and polarization of EF in this case is vertical with the maximum intensity of $4.28*10^4$ V/m.

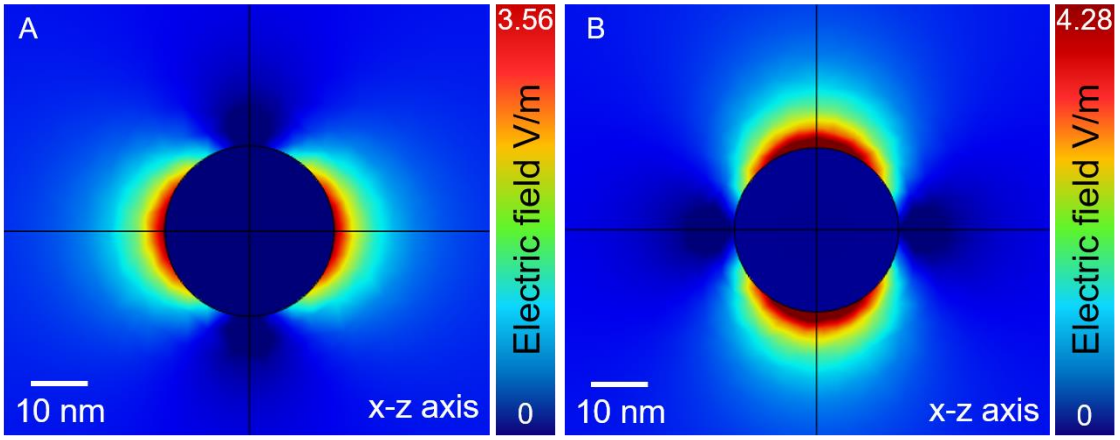

Figure 7. 3D simulation of electric field enhancement around 10 nm radius nanosphere of Au (Johnson and Christy 1972) during the scattering of light: A) Wavelength of 650 nm (red light), light drops from top to bottom, polarization is along horizontal x axis with the maximum of

3.56*10^4 [V/m]; B) Wavelength of 550 nm (yellow-green light), wave goes along x axis and polarization is in vertical z-axis with the maximum of 4.28*10^4 [V/m].

As you can see, value of EF is a bit different for these two situations. This allows us to assume that Localized plasmon resonance is better for 550 nm wave in case of Au (Johnson and Christy 1972) NPs material and the wavelength plays a huge role which we always should consider in experiments and implications, especially in medical diagnostics and therapy.

It should be noted that although the energy harvested exclusively from region of Red light is very small, when combined with other high-energy green and blue photons under one sun conditions, it demonstrates a significantly large amount of solar light harvesting. Longitudinal absorption of Au (Gold) (Johnson and Christy 1972: n,k 0.188-1.937 μm) occurs effectively at 550 nm. Indeed, it absorbs both high-energy yellow-green and low-energy red photons with high absorption coefficient. This leads to more hot electrons as well as red harvesting simultaneously, and hence the high activity is observed. Whereas the extent of such synergistic light absorption is less with other size nanospheres (Fig. 7).

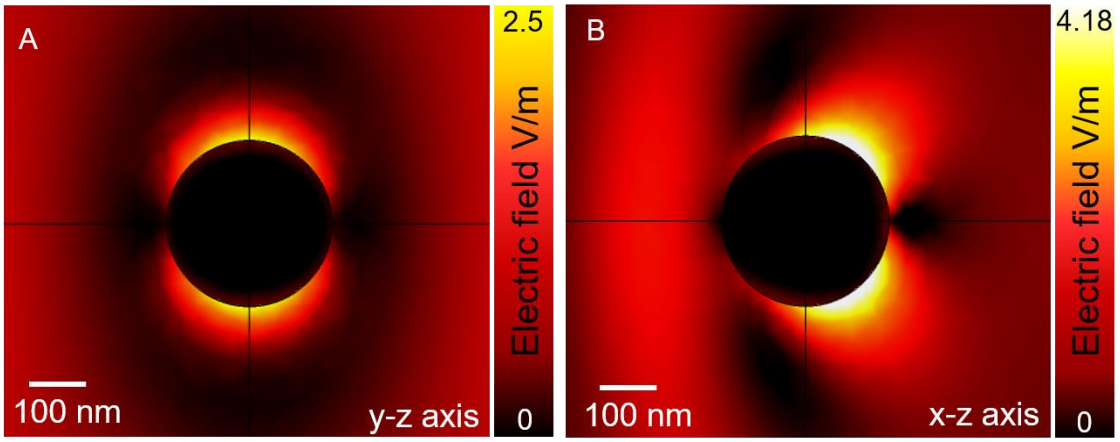

Figure 8. 3D simulated enhancement of electric field around 100 nm radius nanosphere of Au (Johnson and Christy 1972) during the scattering of light with 550 nm wavelength. Wave goes along x axis and polarization is in vertical z-axis: A) y-z axis distribution of electric field with the maximum of 2.5*10^4 [V/m]; B) y-z axis distribution of electric field with the maximum of 4.18*10^4 [V/m].

Some changes in electric field intensity and its distribution around the nanoparticle with the size increasing from 10 nm to 100 nm and making the incidence wave along the X axis with polarization in Z axis were investigated (Fig. 8). Here not only decreasing of EF maximum value but also some changing in EF shape can be observed. In Y-Z axis (Fig. 8 A) maximum intensity drops from 3.56 (Fig. 7 A) to 2.5 V/m and the area of enhancement become weaker and a bit smaller. In X-Z axis profile we can see a slight decrease of EF amplitude from 4.28 (Fig 7 B) to 4.18 V/m. Meanwhile the shape of EF distribution significantly changes and angle of polarization from 90 degrees becomes closer to 45 degrees.

All these factors lead to understanding of NPs size importance which always should be considered in LSPR investigations. Moreover, this knowledge can be used to create some new methods in diagnostics and therapy of tumor cells. But in order to prove the therapeutic effect, it is necessary to conduct studies of the temperature effect which will be described in the following

works.

4. Conclusion

In this research, a lot of reports related to the LSPR and plasmon-induced reactions are analyzed. It is possible to conclude that that more attention should be payed to EF and temperature distribution which are connected not only with the crystallinity structure but also with many other parameters on which are focused in the discussion part.

The size- and wavelength-, dependence with surface EF reaction from surface plasmon resonances on Au NPs have been investigated. Enhancement of electric field is strongly connected with the wavelength of irradiation meanwhile EF distribution depends on the size of nanoparticle. The more NP size is, the more deformation and changing of angle can be observed. This observation is precisely what the simulation results and analyses demonstrate.

The next step is investigation of this plasmon-induced reaction on the single nanocube level with investigation of not only EF dependence but also the power density distribution which are related to the temperature influence taking into account as much as possible of already known studies of this process.

References:

1. Aizpurua, J., Baumberg, J.J., Bowman, R.W., Dubertret, B., Herrmann, L.O., Ithurria, S., Mertens, J., Shi, Y., Sigle, D.O., Tserkezis, C., Yang, H.Y. (2015). Monitoring Morphological Changes in 2D Monolayer Semiconductors Using Atom-Thick Plasmonic Nanocavities. *ACS Nano 2015*. 9. pp. 825−830.

2. Aizpurua, J., Baumberg, J.J., Colli, A., Eiden, A.L., Ferrari, A.C., Huang, F., Lombardo, A., Mertens, J., Milana, S., Sigle, D.O., Sundaram, R.S., Sun, Z., Tserkezis, C. (2013). Controlling Subnanometer Gaps in Plasmonic Dimers Using Graphene. *Nano Lett.* 13. pp. 5033−5038.

3. Barrow, S.J., Baumberg, J.J., Benz, F., Bowman, R.W., de Nijs, B., Chikkaraddy, R., Eiden, A., Ferrari, A., Herrmann, L.O., Mertens, J., Scherman, O.A., Sigle, D.O. (2015). Unfolding the Contents of Sub-nm Plasmonic Gaps Using Normalising Plasmon Resonance Spectroscopy. *Faraday Discuss.* 178. pp. 185−193.

4. Baumberg, J., de Nijs, B., Ding, T., Mertens, J., Sigle, D., Zhang, L. (2015). Controllable Tuning Plasmonic Coupling with Nanoscale Oxidation. *ACS Nano 2015*. 9. pp. 6110−6118.

5. Bing, Zhao, Haibo, Li, Hailong, Wang, Shuping, Xu & Weiqing, Xu. Integrated plasmon-enhanced Raman scattering (iPERS) spectroscopy. [Available at https://www.nature.com/articles/s41598-017-15111-3.pdf?origin=ppub] [Viewed on 12.12.2019].

6. Cao, S.H., Cai, Liu, Q., Li, Y. Q. & W. P. (2012). Surface plasmon-coupled emission: what can directional fuorescence bring to the analytical sciences? *Annu. Rev. Anal. Chem.* 5. pp. 317–336.

7. Cao, S.H. et al. (2014). Label-free aptasensor based on ultrathin-linker mediated hot-spot assembly to induce strong directional fuorescence. *J. Am. Chem. Soc.* 136. pp. 6802–6805.

8. Claverie, J.P., Jin, X., Liu, H., Morales-Guzman, P.I., Razzari, L., Yu, X., Zhang, H., Zhang, J. (2016). Engineering the Absorption and Field Enhancement Properties of Au-TiO2 Nanohybrids via Whispering Gallery Mode Resonances for Photocatalytic Water Splitting. *ACS Nano 2016*. 10. pp. 4496−4503.

9. Codrington, J., Foley, J.J., Fernando, K. and Eldabagh, N. (2017). Unique Hot Carrier Distributions from Scattering-Mediated Absorption. *ACS Photonics 2017*. 4. pp. 552−559.

10. Comesañ a-Hermo, M., Correa-Duarte, M.A., Govorov, A.O., Kong, X.-T., Perez-Lorenzo, M., Rodríguez-Gonzalez, B., Sousa-Castillo, A., Wang, Z. (2016). Boosting Hot Electron-Driven

Photocatalysis through Anisotropic Plasmonic Nanoparticles with Hot Spots in AuTiO2 Nanoarchitectures. *J. Phys. Chem*. 120, pp. 11690−11699.
11. Coronado, Eduardo, Schatz, George C., Kelly, K. Lance and Zhao, Lin Lin. (2003). The Optical Properties of Metal Nanoparticles: The Influence of Size, Shape, and Dielectric Environment. *J. Phys. Chem. B.* Vol. 107. No. 3. pp. 668-677.
12. Foley, J.J., Gray, S.K., Li, Z., Peng, S., Ren, Y., Sun, C.-J., Sun, Y, Wiederrecht, G.P. (2015). Reversible Modulation of Surface Plasmons in Gold Nanoparticles Enabled by Surface Redox *Chemistry*. *Angew. Chem*. 127. pp. 9076−9079.
13. Lombardi, A., Mertens, J., Baumberg, J.J., Scherman, O.A. and Ding, Tao. (2017). Light-Directed Tuning of Plasmon Resonances via Plasmon-Induced Polymerization Using Hot Electrons. *ACS Photonics 2017*. 4. pp. 1453−1458.
14. Neogi, A. et al. (2202). Enhancement of spontaneous recombination rate in a quantum well by resonant surface plasmon coupling. *Phys Rev B.* [Available at https://journals.aps.org/prb/abstract/10.1103/PhysRevB.66.153305] [Viewed on 10.11.2019]